Symbiont dynamics during the blood meal of Ixodes ricinus nymphs differ according to their sex

Romain Daveu, Cindy Laurence, Agnès Bouju-Albert, Davide Sassera, Olivier
Plantard

HAL Id: hal-03229083
https://hal.inrae.fr/hal-03229083

1 Symbiont dynamics during the blood meal of *Ixodes*

2 *ricinus* nymphs differ according to their sex

3

4 Romain Daveu[ab], Cindy Laurence[a], Agnès Bouju-Albert[ac], Davide Sassera[b], Olivier Plantard[a]

5 [a] INRAE, Oniris, BIOEPAR, 44300, Nantes, France

6 [b] Department of Biology and Biotechnology "L. Spallanzani", University of Pavia, Pavia, Italy

7 [c] INRAE, Oniris, SECALIM, 44300, Nantes, France

8

9 Corresponding author:

10 olivier.plantard@inrae.fr

11

14

15 ABSTRACT

16

17 Ticks harbour rich and diverse microbiota and, among the microorganisms associated with

18 them, endosymbionts are the subject of a growing interest due to their crucial role in the

19 biology of their arthropod host. *Midichloria mitochondrii* is the main endosymbiont of the

20 European tick *Ixodes ricinus* and is found in abundance in all *I. ricinus* females, while at a

21 much lower density in males, where it is even absent in 56% of the individuals. This

22 endosymbiont is also known to increase in numbers after the blood meal of larvae, nymphs

23 or females. Because of this difference in the prevalence of *M. mitochondrii* between the two

24 sexes, surveying the density of these bacteria in nymphs that will become either females or

25 males could help to understand the behaviour of *Midichloria* in its arthropod host. To this

aim, we have set up an experimental design by building 3 groups of unfed nymphs based on their scutum and hypostome lengths. After engorgement, weighing and moulting of a subset of the nymphs, a significant difference in sex-ratio among the 3 groups was observed. In parallel, *Midichloria* load in individual nymphs was quantified by qPCR both before and after engorgement.

No difference in either body mass or *Midichloria* load was observed at the unfed stage, but following engorgement, both features were significantly different between each size group. Our results demonstrate that symbiont dynamics during nymphal engorgement is different between the two sexes, resulting in a significantly higher *Midichloria* load in nymphs that will become females. The consequences of those findings on our understanding of the interplay between the endosymbiont and its arthropod host are discussed.

1 INTRODUCTION

Ticks are obligate hematophagous ectoparasites, vectors of numerous pathogens for both humans and animals (Jongejan and Uilenberg, 2004; Parola and Raoult, 2001). Beside pathogens, ticks harbour a diverse microbiome including commensal and symbiotic microorganisms (Bonnet et al., 2017; Duron et al., 2017). This is a common situation in arthropods, as most species are the host of various bacterial symbionts that can be transmitted transovarially to the progeny (Bennett and Moran, 2015; Wernegreen, 2012). During their long-lasting co-evolution with their arthropod hosts, symbionts have developed strategies to persist and multiply within their host. Some are obligate mutualists, essential for host fitness, whereas others may be facultative, allowing for example a better survival in adverse environmental conditions, providing resistance to natural enemies or manipulating host reproduction (Bennett and Moran, 2015; Cordaux et al., 2011; Engelstädter and Hurst, 2009; Haine, 2008; Oliver et al., 2003; Vorburger et al., 2010).

At least ten genera of symbionts have been reported in ticks, three of them being exclusive to ticks, *i.e. Coxiella*-like endosymbionts, *Francisella*-like endosymbionts and *Midichloria* (Bonnet et al., 2017; Díaz-Sánchez et al., 2019; Duron et al., 2017; Narasimhan and Fikrig, 2015). The obligatory role of some symbionts on tick fitness has been shown by removal through antibiotics (Ben-Yosef et al., 2020; Duron et al., 2018; Guizzo et al., 2017; Zhang et al., 2017; Zhong et al., 2007). In addition, a role as vitamin B provider has been demonstrated in the case of *Francisella*-like endosymbionts of *Ornithodoros moubata* (Duron et al., 2018).

Candidatus Midichloria mitochondrii (hereafter *M. mitochondrii*) (Alphaproteobacteria: Rickettsiales: Midichloriaceae) is the main and most abundant symbiont of *I. ricinus,* the most common tick species in Europe (Guizzo et al., 2020; Sassera et al., 2006). Like all hard-tick species, *I. ricinus* displays a four-stage life cycle (larva, nymph, adult and egg). Each moulting (*i.e.* from larva to nymph and from nymph to adult) occurs after a blood meal, whereas egg-laying is conditioned by both female fertilisation and a third and final blood meal. *Midichloria mitochondrii* resides principally in oocyte cells (Beninati et al., 2004; Sassera et al., 2006; Zhu et al., 1992) but also, at a much smaller density, in salivary glands, Malpighian tubules and tracheae (Olivieri et al., 2019). Its density is also highly variable according to life stage and engorgement status, with a considerable bacterial growth observed following a blood meal in larvae, nymphs and females (Sassera et al. 2008). The bacterium exhibits a unique feature among symbionts as it resides within the host's mitochondrial intermembrane (Beninati et al., 2004; Stavru et al., 2020). This alphaproteobacterium is ~100% prevalent in females and immatures (Aivelo et al., 2019), while a medium prevalence in males (~40%) has been observed (Lo et al., 2006; Sassera et al., 2006). However, despite the high prevalence of these endosymbionts in *I. ricinus*, the consequences of the presence of *M. mitochondrii* in its arthropod hosts remain to be established experimentally.

78   Considering that (i) in *I. ricinus* there is a marked difference in *M. mitochondrii* prevalence

79   between sexes, (ii) vertical transmission of *M. mitochondrii* has been demonstrated as it has

80   been found in egg masses (Lo et al., 2006; Sassera et al., 2008), and (iii) an extensive

81   variability of *M. mitochondrii* density between nymph individuals has been reported,

82   especially in fed nymphs (Sassera et al., 2008), we designed the present study to investigate

83   the dynamics of *M. mitochondrii* in this sexually immature stage of *I. ricinus*.

84   Such information could help us understand the interplay between the host tick and its

85   symbiont *M. mitochondrii*. A first hypothesis could be that *M. mitochondrii* presence or

86   density is determined by the genetic sex of ticks (in *I. ricinus*: XY for males, XX for females;

87   Oliver, 1977) with a lower density or absence of *M. mitochondrii* in immature stages with a Y

88   chromosome (*i.e.* nymphs that will become males). An additional hypothesis - not exclusive

89   to the first one - could be that symbiont cells are restricted to the ovary and absent in the

90   testes (the two organs being at a primordial stage in unfed nymphs but reaching a larger size

91   following the blood meal and the metamorphosis process (Balashov, 1972). The number of

92   endosymbionts may thus increase according to ovary development during ontogenic

93   processes (while it may not increase following testes development). Note that tissue/organ

94   location of *M. mitochondrii* has been investigated to date only in adults, due to the smaller

95   size of immature stages such as nymphs (but see Epis et al., 2013). As *I. ricinus* do not

96   show any sexual dimorphism at the nymphal stage while unfed, nymphs that will become

97   either females or males cannot be identified prior to engorgement. Moreover, to date, no

98   sexual genetic marker exists for ticks, despite ongoing investigations for whole genome

99   sequencing of several *Ixodes* species (Gulia-Nuss et al., 2016; Jia et al., 2020; Murgia et al.,

100   2019). To investigate the dynamics of *M. mitochondrii* in nymphs that will become either

101   males or females, we set up an experimental design to examine groups of nymphs based on

102   morphometric characteristics enabling to obtain different sex ratios in those groups. We then

103   investigated *Midichloria* load in the nymphs of these groups, both before and after

104   engorgement.

105 Finally, we will discuss the consequences of our findings concerning the evolution of

106 *Midichloria* load during nymph development on our understanding of *Midichloria* biology and

107 its interplay with its arthropod host.

108

2 MATERIALS and METHODS

2.1. Study design

111 To discriminate between unfed nymphs that will become males *versus* females, we took

112 advantage of a known size dimorphism (using body mass as a proxy) observed in nymphs

113 fed at repletion that exhibit a marked bimodal distribution, with the heavier ones becoming

114 females, and the lighter becoming males (Dusbábek, 1996, Kahl et al., 1990). This

115 difference in body mass or morphometric features (such as idiosoma, scutum or hypostome

116 lengths) between fed nymphs that will become males *versus* females is also present in unfed

117 nymphs, but an extensive overlap is observed between the two distributions (that are not

118 bimodal; Dusbabek 1996) preventing sex determination of individual nymphs prior to

119 engorgement. In the present study, we built size groups based on morphometric features

120 (*i.e.* hypostome and scutum lengths), with a hypothesised different sex-ratio, then we

121 proceeded to the engorgement of the different groups separately, collecting a portion of

122 unengorged and engorged nymphs prior to their moult to assess their *M. mitochondrii* load

123 by qPCR (Fig. 1).

2.2. *Ixodes ricinus* ticks and morphological measurements

125 250 wild unfed *I. ricinus* nymphs were collected in January 2014 using the dragging method

126 in Chizé forest, France (46°08'31.5"N, 0°25'22.5"W). Ticks were maintained in desiccators at

127 20°C, 90% relative humidity (with a saturated magnesium sulfate solution), 12 hrs dark:12

128 hrs light, until further use. Using a stereo microscope (Nikon SMZ800), a picture of each

129   individual nymph was taken (Fig. 2). With the help of a 1 mm micrometric blade allowing to

130   provide the scale of each picture, each nymph was characterized for the length of its scutum

131   (rigid, sclerotised plate on the anterior dorsal surface, just posterior to the capitulum) and

132   hypostome (harpoon-like structure forming part of the mouthparts of ticks). Because the

133   posterior end of the hypostome is difficult to locate due to the slope of the tectum, the length

134   measured for the hypostome also includes the base of the capitulum, up to the cornua which

135   are easily identifiable.

136

137   Body mass of both unfed and engorged nymphs was measured with an ultra microbalance

138   (Sartorius, Cubis MSA2). Hypostome and scutum lengths were used to divide the nymph

139   population into three initial groups (small, medium and large size; $x_{1,S}$, $x_{1,M}$ and $x_{1,L}$; Fig. 1)

140   with an equal number of individuals. Ticks of each size group were then divided into three

141   treatment lots (Fig. 1; x_2, x_3, x_4), and submitted to the following: (a) DNA extraction and

142   qPCR targeting *Midichloria mitochondrii* on individual unfed nymphs (Fig. 1; $x_{2,S}$, $x_{2,M}$ and

143     $x_{2,L}$), engorgement of nymphs on a gerbil (Fig. 1; $x_{3,S}$, $x_{3,M}$, $x_{3,L}$), followed by either (b) DNA

144   extraction and qPCR of individual engorged nymphs (Fig. 1; $x_{4,S}$, $x_{4,M}$, $x_{4,L}$), or (c) molting to

145   establish sex ratios in each of the 3 size groups (Fig. 1; $x_{5,S}$, $x_{5,M}$, $x_{5,L}$).

146

147   2.3. *Ixodes ricinus* ticks and morphological measurements

148   The protocol was approved by the Ethics Committee for Animal Experiments of the Pays de

149   la Loire region (CEEA PdL 06) (Permit Number: 2015-29). Engorgement on gerbils was

150   conducted as described in Bonnet et al. (2007). In short, for each of the size groups (small,

151   medium and large), 47 or 50 nymphs were put on an individual gerbil. The 3 gerbils were

152   each put on a shelf above a tray of water, in a separate box. Once engorged, ticks fallen in

153   the water were collected twice a day. It should be noted that the information available for

154   each individual nymph (id est body mass, hypostome and scutum lengths) was lost after

155 engorgement because each tick can not be identified and surveyed individually during

156 engorgement (only the group information is retained).

157

2.4. Quantitative PCR to determine *Midichloria mitochondrii* density

158 ## 2.4. Quantitative PCR to determine *Midichloria mitochondrii*

159 density

160 The ratio between the qPCR quantifications of the symbiont gene gyrase B (*gyrB*) and the

161 tick calreticulin gene (*cal*) allows to estimate the *Midichloria mitochondrii* density, *i.e.* the

162 number of bacteria per tick cell. DNA was extracted using the NucleoSpin Tissue DNA kit

163 (Macherey-Nagel) according to manufacturer's instructions after crushing the ticks using a

164 pestle. As previously described (Sassera et al., 2008)*, M. mitochondrii* load was quantified

165 with a SYBR Green Kit (Sigma-Aldrich) using the ratio of single-copy genes - DNA *gyrB* for

166 the bacteria (primer forward CTTGAGAGCAGAACCACCTA and reverse

167 CAAGCTCTGCCGAAATATCTT; amplicon 125 bp) by *cal* gene for the host (primers

168 ATCTCCAATTTCGGTCCGGT and TGAAAGTTCCCTGCTCGCTT; amplicon 109 bp). The

169 results were compared for single nymphs with those of serial dilutions of purified cloned

170 pGEM-T easy plasmid vector (Promega corporation) with known copy number to determine

171 the number of bacteria per host cell at each run. The PCR amplification of the *gyrB* and *cal*

172 genes was as follows: 95°C for 2 min, 40 cycles at 95°C for 15 s and at 60°C for 30 s, and

173 melt curve from 55°C to 95°C with increasing increments of 0.5°C per cycle.

2.5. Determination of the sex ratio in each nymphs group

175 For each size group (Fig. 1; $x_{5,S}$, $x_{5,M}$, $x_{5,L}$), after engorgement, the nymphs were weighed.

176 Once ranked according to their body mass, one out of two engorged nymph was selected (to

177 form groups with the same body mass distribution) and was maintained in a desiccator with

7

178 a saturated magnesium sulfate solution (90% relative humidity) and 20°C, and checked

179 every day until metamorphosis, at which point their sex could be determined.

2.6. Statistical Analysis
180

181 All analyses were performed with R (v3.6.2) within the RStudio IDE (v1.2), using ggplot2

182 (Wickham, 2016), dplyr (Wickham et al., 2020), tidyr (Wickham and Henry, 2020), FSA (Ogle

183 et al., 2020), cowplot (Wilke, 2019) and stats (R Core Team, 2020) packages. The density

184 curves were first built with the built-in density function then using the geom_density function

185 of ggplot2 which uses the kernel density estimation method and relies on the built-in density

186 function implemented in R. Modes were obtained using a homemade function determining

187 the maxima of each curve. The sample size of each nymphs size group (Fig. 1; $x_{1,S}$, $x_{1,M}$,

188 $x_{1,L}$) was restricted by the maximal number of ticks that can be deposited on an individual

189 gerbil (80 nymphs per gerbil). Moreover, each nymph size group was subsequently split into

190 thirds (Fig. 1; for example the smallsized group was split into $x_{2,S}$, $x_{4,S}$, $x_{5,S}$). Finally, the

191 qPCR method is a destructive method requiring the destruction of individual nymphs (these

192 individuals could not be used to later determine their sex). For all these reasons, the sample

193 size of each group considered is below 30 and thus nonparametric statistical tests were

194 performed.The distribution equality or non-equality was determined using a Kruskal-Wallis

195 test followed by a pairwise Dunn test, or a Wilcoxon rank sum test when only two groups

196 were compared.

197

3 RESULTS

3.1. UNFED NYMPHS

3.1.1. Use of hypostome and scutum lengths to build nymph groups exhibiting different sex-ratios

Two criteria - hypostome and scutum lengths (Fig. 2) - were chosen to sort unfed nymphs in three groups (small, medium and large), as shown by the different coloured dots in Fig. 3. Among all measurements, the hypostome measured between 0.500 and 0.733 mm with a mean length of 0.636±0.083 mm whereas the scutum gauged between 1.180 and 1.700 mm with a mean length of 1.494±0.043 mm. These morphometric variables exhibited a correlation (R^2 = 0.2819, P < 0.01). An equal number of individuals were split into three batches according to their scutum and hypostome length (see Fig. 1; $x_{1,S}$, $x_{1,M}$, $x_{1,L}$; Table 1).

3.1.2. Nymph body mass before engorgement

Before engorgement, the tick body mass showed a normal distribution (102.6 - 320.1 µg, mean = 199.8±35.3 µg, ±SD), (Fig. S1). Tick body mass was lowest in the small-sized group (mean = 174.5±29.1 mg, $x_{1,S}$ = 65) average in the medium-sized group (mean = 203.9±26.8 mg, $x_{1,M}$ = 65), and highest in the large-sized group (mean = 221.1±32.8 mg, $x_{1,L}$ = 65). Although the 3 distributions were significantly different (Kruskal-Wallis test P < 1e-14), an extensive overlap among the 3 distributions is observed.

3.1.3. Symbiont density in unfed nymphs

In unfed nymphs, *M. mitochondrii* density fluctuated from no bacteria detected to 5.63 bacteria per host cell (mean 7.3e-01±1.21) (Fig. 4). The *gyB*/*cal* ratio of the small-sized nymphs (mean = 0.58±1.39, $x_{2,S}$ = 18) presented the highest heterogeneity of symbiont density. Values were more uniform for the large-sized nymphs (mean = 0.85±1.01, $x_{2,L}$ = 15),

223   with the *gyrB*/*cal* ratio clearly close to 1 bacterium per cell (except for one outlier) (Fig. 4).

224   Medium-sized nymphs (mean = 0.77±1.24, $x_{2,M}$ = 15) appeared to cluster in two density

225   groups, one around 0.001 and another around 1 bacterium per host cell. At this unfed nymph

226   stage, the symbiont densities of the 3 size groups were not significantly different: none of the

227   size groups displayed a symbiont density higher than the other (Kruskal-Wallis test, P =

228   0.16).

229   # 3.2. FED NYMPHS

230   **3.2.1. Determination of sex ratio in each nymph size group**

231   After moulting of individual engorged nymphs of known body mass, we obtained males and

232   females for each size group as described in Table 1. Mortality rate was not found to be

233   significantly different between each size group. The small-sized group exhibited a majority of

234   males (11 males, 2 females) whereas the large-sized group exhibited a majority of females

235   (15 females, 3 males). It should be noted that although the sex-ratios are different among

236   the 3 groups (*i.e.* 85% *vs* 17% of males; test of given proportion, p-value < 0.001), both the

237   small-sized and the large-sized groups contained individuals of both sexes. Regarding the

238   body mass of engorged nymphs, nymphs that became male were significantly lighter than

239   nymphs that became female (Fig. 5; Wilcoxon rank sum test P<1e-08).

240

241   After having merged all three size groups, the distribution of the body mass density

242   displayed a bimodal pattern, with two clearly distinct modes (mode 1 = 2.79 mg; mode 2 =

243   4.75 mg) (Fig. 6). These last results allowed us to introduce a new variable, the predicted

244   sex, determined according to the body mass of the engorged nymphs. Therefore, we

245   inferred the predicted sex of each engorged nymph based on its body mass considering a

246   threshold value between the two sexes set to 3.78 mg. This threshold corresponded to the

247   minimal value observed between the two distributions (see the vertical line in Fig. 6).

248

249 The observed body mass of engorged nymphs for the small-sized group ranged from 2.16 to

250 5.36 mg, with a mean of 3.12±0.84 mg (Fig. 7), exhibiting a bimodal distribution (Fig S2a)

251 with the first (major) mode around 2.70 mg (25 individuals; predicted sex male) and the

252 second (minor) mode around 4.60 mg (6 individuals; predicted sex female).

253 The body mass for the medium-sized group ranged from 2.28 to 6.21 mg (Fig. 7) (mean =

254 3.81±1.01 mg) with a bimodal distribution (Fig. S2b). The first mode corresponded to 18

255 individuals (mean body mass: 2.90 mg; predicted sex male) while the second mode

256 corresponded to 18 nymphs (mean body mass: 4.60 mg; predicted sex female), with thus a

257 balanced size of the 2 groups corresponding to the 2 modes.

258 The body mass for the large-sized group ranged from 2.48 to 6.73 mg (mean = 4.55±1.03

259 mg) (Fig. 7), with a bimodal distribution (Fig. S2c), the first (minor) mode with a mean around

260 2.90 mg (8 nymphs; predicted sex male) and the second (major) mode around 4.80 mg (29

261 nymphs; predicted sex female).

262 Without considering those bimodal distributions for each size group, the median size was

263 2.84 mg for the small-sized group, 3.6 mg for the medium-sized group and 4.78 mg for the

264 large-sized group. Those 3 medians of the different size groups were significantly different

265 (Kruskal-Wallis test, $P < 1e-06$), the comparisons small-medium, medium-large and small-

266 large were also significantly different (post-hoc Dunn's test, P-values respectively below 1e-

267 03, 1e-03 and 1e-07).

268 The density curves based on the individuals with a predicted sex clearly correspond to two

269 gaussian distributions with different parameters (male mode = 2.74 mg; female mode = 4.79

270 mg) (Fig. S3).

271

272 **3.2.2. Symbiont density in fed nymphs**

273 A total of 106 (72.1 %, n = $x_{3,S} + x_{3,M} + x_{3,L}$ = 147; Fig. 1) nymphs engorged successfully.

274 Among those 106 engorged nymphs, a subset of 54 (16, 19 and 19 from the small, medium

275 and large-sized groups respectively; Fig. 1; $x_{4,S}$, $x_{4,M}$ and $x_{4,L}$) were crushed, DNA was

276 extracted and the symbiont density was quantified.

278 The *gyrB/cal* ratio for the small-sized group ranges from 2.2e-04 to 1.9, with a mean of

279 0.34±0.59 (Fig 8, S4a), exhibiting a bimodal distribution with the first mode around 1e-02 (11

280 individuals, predicted sex male; one *gyrB* value was null and cannot therefore be included in

281 the figure) and the second mode around 1 (5 individuals, 3 predicted sex female and 2

282 predicted sex male). The ratio for the medium-sized group ranges from 5.6e-03 to 2.0 (Fig.

283 8, S4b) (mean = 0.69±0.73), with a bimodal distribution, the first being around 1e-02 (8

284 individuals, predicted sex: male) and the second one being around 1 (8 individuals, predicted

285 sex: female). The *Midichloria* density for the large-sized group ranges from 1.8e-03 to 7.6

286 (mean = 2.3±2.6) (Fig. 8, S4c), and exhibits a first mode at 1e-02 (3 individuals, predicted

287 sex: male) and a second mode at 1 (16 individuals, predicted sex: female, except for one

288 individual). The three groups were significantly different (Kruskal-Wallis test, P-value = 0.01),

289 however only the small and large-sized groups were significantly different (post-hoc Dunn's

290 test, P-value = 0.0054).

291

292 The body mass displayed a significant correlation with the log10 of *Midichloria* density

293 (Spearman's rank correlation, rho = 0.8249104, P<1e-11) (Fig. 9). Two distinct groups can

294 be recognized, with the first one (blue ellipse in Fig. 9) corresponding to nymphs with the

295 smallest body mass (predicted sex: male) and exhibiting the lowest gyrB/cal ratios, while the

296 other cluster (red ellipse) gathered nymphs with the highest body mass (predicted sex:

297 female) and the highest *gyrB*/*cal* ratio.

298 4 DISCUSSION

299 4.1. Validation of groups of unfed nymphs with different sex-ratios based on

300 morphometric features

301 To compare the growth of *M. mitochondrii* during engorgement in nymphs that will become

302 either males or females, it is necessary to identify *a priori* (*i.e.* before engorgement) the sex

of nymphs, using a non-destructive method (allowing future engorgement). Our strategy to

build 3 groups of unfed nymphs based on morphological features (using scutum and

hypostome lengths, as suggested by Dusbabek et al., 1996) and exhibiting different sex-

ratios was successful. Following engorgement, we validated that the sex-ratios among the 3

groups (initially formed according to those morphological features) were significantly

different. The differences in sex-ratio among the 3 groups (of unfed nymphs $i.e.$ $x_{1,S}$, $x_{1,M}$ and

$x_{1,L}$) were also confirmed by the engorged nymphs body mass ($x_{3,S}$, $x_{3,M}$, $x_{3,L}$) where the

sample size of each of the two modes (corresponding to males [the lightest] and females

[the heaviest] respectively) are clearly different among the 3 groups (Fig. 7 and S2). Indeed,

while the overlap between the body mass distribution of unfed nymphs is too broad to allow

sex determination (as it did not exhibit a bimodal pattern; Fig. S1), once engorged, nymphs

that will become females are significantly heavier than nymphs that will become males, with

no overlap between the two body mass distributions observed where the highest body mass

for an engorged male-to-be nymph was 3.60 mg (n = 22) and the smallest body mass for an

engorged female-to-be nymph was 3.92 mg (n = 25) (Fig. 5). This last observation confirms

previously published results on $I.$ $ricinus$ (Dusbábek et al., 1995, 1994; Kahl et al., 1990).

Similar observations have been made on other tick species ($I.$ $rubicundus$ (Belozerov et al.,

1993), $I.$ $scapularis$ (Hu and Rowley, 2000), $Amblyomma$ $americanum$, $A.$ $maculatum$,

$Dermacentor$ $variabilis$, $Rhipicephalus$ $sanguineus$ sensu lato (Nagamori et al., 2019)),

however this is not strictly the case for all tick species (see for instance $D.$ $andersoni$

(Nagamori et al., 2019). Although the differences based on morphological features and

engorged body mass between nymphs that will become either males or females were

already known (Dusbabek et al., 1996), we are not aware of any studies on ticks published

to date that have been able to build groups exhibiting different sex-ratios before

engorgement. This strategy that we have validated through our experimental approach can

now be used to investigate not only symbiont load in sexually immature stages, but any

other biological traits that would aim to compare nymphs that will become males with those

going on to become females.

4.2. Use of *Midichloria* load in individual nymph to determinate their sex

Regarding unfed nymphs, there are no significant differences in *Midichloria* load between the three groups of nymphs (Fig. S1). Thus, the overlap in *Midichloria* load between nymphs that will become males and those that will become females is too extensive to predict the sex of adult *I. ricinus*. Firstly, the reduced sample size of our data set may partly explain the absence of significant differences observed among the 3 groups. However, even with a larger sample size, it would be difficult to assign a sex to an individual nymph with a high level of confidence, because intermediate values of the *gyrB*/*cal* ratio (*e.g.* 1e-2) are observed in the small-sized group of nymphs (Fig. 4). Secondly, the lack of significant differences among the 3 groups of unfed nymphs could be due to the heterogeneity in symbiont load among individual nymphs within a given sex, as suggested by the wide range of *gyrB*/*cal* ratios observed within a given group (Fig. 4). This inter-individual variability may be explained by differences in primordium development among individuals at such an early stage of the development of the gonad tissue.

Concerning fed nymphs, even if there is a clear difference in *Midichloria* load between the nymphs that will become males and those that will become females (see the ellipses in Fig. 9), there is still an overlap of the 2 distributions of endosymbiont density. The addition of the information corresponding to engorgement body mass is thus needed to predict whether an individual nymph will become a male or a female.This may be due to interindividual variations in *Midichloria* load prior to engorgement (as observed in Duron et al., 2018). Even if the engorgement is clearly responsible for an increasing difference in *Midichloria* load according to sex, those differences are not sufficient to identify the sex of an individual nymph.

4.3. Evolution of *Midichloria* load in nymphs following engorgement according to their sex

358 Our study aimed to obtain an accurate comparison of the *M. mitochondrii* density in *I. ricinus*

359 nymphs before and after engorgement and in nymphs that will become either males or

360 females. The rationale was based on the fact that *Midichloria* symbionts are found at a high

361 density in females and are at a very low density - or even completely absent - in males. Until

362 now, only limited data were available to establish the dynamics of this symbiont following the

363 engorgement of its arthropod host. Only the study by Sassera et al. (2008) partially

364 investigated this point and revealed an extensive interindividual heterogeneity of *Midichloria*

365 load, especially in fed nymphs. First, our results clearly demonstrate that *Midichloria* load is

366 significantly different in engorged nymphs that will become males compared to those

367 becoming females, with higher *Midichloria* loads in engorged nymphs that will become

368 females (Fig. 8, 9, S4 and S5). The extensive inter-individual heterogeneity of *Midichloria*

369 load observed in fed nymphs investigated by Sassera et al. (2008) could thus be due to the

370 mixture of both males and females, each harbouring a highly different Midichloria load.

371 Those results also suggest that the dynamics of *Midichloria* in its arthropod host are different

372 according to its sex. As with all intracellular vertically transmitted symbionts (Vautrin and

373 Vavre, 2009), males are a dead end for *Midichloria*. Moreover, in the particular case of

374 hematophagous arthropods, as *I. ricinus* males only very rarely bite vertebrates (Balashov,

375 1972), they probably have limited or null participation in potential horizontal transmission of

376 *Midichloria* via the vertebrate host. Such a horizontal transmission may be possible in the

377 case of females, as suggested by the observation of this symbiont in salivary glands and

378 even in vertebrate blood during an experimental investigation (Cafiso et al. 2018) and also

379 by the incomplete co-cladogenesis between the symbiont and the arthropod phylogenies (Al-

380 Khafaji et al., 2019; Epis et al., 2008; Mariconti et al., 2012). The observed differences in

381 *Midichloria* load between nymphs that will become males *versus* females may thus be due to

382 the different development of gonad primordia (*i.e.* testes in males *versus* ovaries in females).

383 As *Midichloria* is known to be especially abundant in ovarian tissue (Olivieri et al., 2019;

384 Sacchi et al., 2004), the ovarian primordium in fed nymphs that will become females may be

385 more developed than in unfed nymphs and thus may explain the increase in *Midichloria* load

386　between unfed and fed nymphs. Because the difference in Midichloria load between males

387　and females nymphs was observed only in fed nymphs and not in unfed nymphs, we argue

388　that the sole presence of the Y chromosome in males nymphs is not sufficient to explain the

389　observed difference in Midichloria density (otherwise it would also be observed in unfed

390　nymphs). The positive relationship between body mass and *gyrB/cal* ratio observed in figure

391　9 could be interpreted as linear (*id est* "whatever the sex of the nymphs") and resulting from

392　the fact that more metabolite are available in nymphs that will become females due to their

393　larger blood meal. Alternatively, the 2 ellipses in the figure 9 (corresponding to the males

394　and females-to-be nymphs respectively) could also be considered as exhibiting each a

395　different slope, hence suggesting a different (non-linear) mechanism involved in *Midichloria*

396　multiplication between the 2 sexes

397　Like other maternally transmitted symbionts, when located in the somatic line, the bacteria

398　may exhibit a reduced multiplication relative to the one observed in the germinal line. Indeed,

399　only the tissues corresponding to the germinal line contribute to the vertical transmission of

400　the symbiont in its host offspring (Christensen et al., 2019). Nymph dissection to extract

401　ovarian primordia and quantify *Midichloria* in this tissue could be conducted to investigate if

402　there is an increasing density of *Midichloria* in those cells or if the load increases due to the

403　development of these primordia and cell division. Finally, additional investigations, such as

404　the comparison of the dynamics of *Midichloria* in male *versus* female adult tissues (including

405　gonads), before and after engorgement, could also be conducted to provide new information

406　concerning the different fates of the symbiont between the two sexes. .

407　Beside the potential role of endosymbionts as vitamin providers for their arthropod host, it

408　has been recently demonstrated that the endosymbionts *Midichloria* sp., in combination with

409　the *Francisella*-like endosymbionts, are involved in the vectorial competence of *Rickettsia*

410　*parkeri* by *Amblyomma maculatum* (Budachetri et al., 2018). We thus argue that a better

411　knowledge of the multiplication pattern of endosymbionts in immature stage could also be

412　useful to understand the role of *Midichloria* and its consequences on tick biology as well as

413　the interplay between the symbiont and its arthropod host.

Declarations of interest:

Acknowledgements

Funding

References

Aivelo, T., Norberg, A., Tschirren, B., 2019. Bacterial microbiota composition of *Ixodes ricinus* ticks: the role of environmental variation, tick characteristics and microbial interactions. PeerJ 7, e8217. https://doi.org/10.7717/peerj.8217

Al-Khafaji, A.M., Clegg, S.R., Pinder, A.C., Luu, L., Hansford, K.M., Seelig, F., Dinnis, R.E., Margos, G., Medlock, J.M., Feil, E.J., Darby, A.C., McGarry, J.W., Gilbert, L., Plantard, O., Sassera, D., Makepeace, B.L., 2019. Multi-locus sequence typing of *Ixodes ricinus* and its symbiont *Candidatus* Midichloria mitochondrii across Europe reveals evidence of local co-cladogenesis in Scotland. Ticks Tick-Borne Dis. 10, 52–62. https://doi.org/10.1016/j.ttbdis.2018.08.016

Balashov, Y.S., 1972. Bloodsucking ticks (Ixodoidea)-vectors of disease in man and animals. Misc. Publ. Entomol. Soc. Am. 8, 161-376

Ben-Yosef, M., Rot, A., Mahagna, M., Kapri, E., Behar, A., Gottlieb, Y., 2020. Coxiella-Like Endosymbiont of *Rhipicephalus sanguineus* Is Required for Physiological Processes During Ontogeny. Front. Microbiol. 11. https://doi.org/10.3389/fmicb.2020.00493

Beninati, T., Lo, N., Sacchi, L., Genchi, C., Noda, H., Bandi, C., 2004. A Novel Alpha-Proteobacterium Resides in the Mitochondria of Ovarian Cells of the Tick Ixodes ricinus. Appl. Environ. Microbiol. 70, 2596–2602. https://doi.org/10.1128/AEM.70.5.2596-2602.2004

Bonnet, S., Jouglin, M., Malandrin, L., Becker, C., Agoulon, A., L'hostis, M., Chauvin, A., 2007. Transstadial and transovarial persistence of *Babesia divergens* DNA in *Ixodes ricinus* ticks fed on infected blood in a new skin-feeding technique. Parasitology 134, 197–207. https://doi.org/10.1017/S0031182006001545

Bonnet, S.I., Binetruy, F., Hernández-Jarguín, A.M., Duron, O., 2017. The Tick Microbiome: Why Non-pathogenic Microorganisms Matter in Tick Biology and Pathogen Transmission. Front. Cell. Infect. Microbiol. 7. https://doi.org/10.3389/fcimb.2017.00236

463 Budachetri, K., Kumar, D., Crispell, G., Beck, C., Dasch, G., Karim, S., 2018. The tick

464   endosymbiont *Candidatus* Midichloria mitochondrii and selenoproteins are essential

465   for the growth of *Rickettsia parkeri* in the Gulf Coast tick vector. Microbiome 6, 141.

466   https://doi.org/10.1186/s40168-018-0524-2

467 Christensen, S., Camacho, M., Sharmin, Z., Momtaz, A.J.M.Z., Perez, L., Navarro, G.,

468   Triana, J., Samarah, H., Turelli, M., Serbus, L.R., 2019. Quantitative methods for

469   assessing local and bodywide contributions to *Wolbachia* titer in maternal germline

470   cells of *Drosophila*. BMC Microbiol. 19, 206. https://doi.org/10.1186/s12866-019-

471   1579-3

472 Díaz-Sánchez, S., Estrada-Peña, A., Cabezas-Cruz, A., de la Fuente, J., 2019. Evolutionary

473   Insights into the Tick Hologenome. Trends Parasitol. 35, 725–737.

474   https://doi.org/10.1016/j.pt.2019.06.014

475 Duron, O., Binetruy, F., Noël, V., Cremaschi, J., McCoy, K.D., Arnathau, C., Plantard, O.,

476   Goolsby, J., Pérez de León, A.A., Heylen, D.J.A., Van Oosten, A.R., Gottlieb, Y.,

477   Baneth, G., Guglielmone, A.A., Estrada-Peña, A., Opara, M.N., Zenner, L., Vavre, F.,

478   Chevillon, C., 2017. Evolutionary changes in symbiont community structure in ticks.

479   Mol. Ecol. 26, 2905–2921. https://doi.org/10.1111/mec.14094

480 Duron, O., Morel, O., Noël, V., Buysse, M., Binetruy, F., Lancelot, R., Loire, E., Ménard, C.,

481   Bouchez, O., Vavre, F., Vial, L., 2018. Tick-Bacteria Mutualism Depends on B

482   Vitamin Synthesis Pathways. Curr. Biol. 28, 1896-1902.e5.

483   https://doi.org/10.1016/j.cub.2018.04.038

484 Dusbábek, F., 1996. Nymphal sexual dimorphism in the sheep tick *Ixodes ricinus* (Acari:

485   Ixodidae). Folia Parasitol. (Praha) 43, 75–79.

486 Epis, S., Mandrioli, M., Genchi, M., Montagna, M., Sacchi, L., Pistone, D., Sassera, D., 2013.

487   Localization of the bacterial symbiont *Candidatus* Midichloria mitochondrii within the

488   hard tick *Ixodes ricinus* by whole-mount FISH staining. Ticks Tick-Borne Dis. 4, 39–

489   45. https://doi.org/10.1016/j.ttbdis.2012.06.005

490 Epis, S., Sassera, D., Beninati, T., Lo, N., Beati, L., Piesman, J., Rinaldi, L., McCOY, K.D.,

19

491   Torina, A., Sacchi, L., Clementi, E., Genchi, M., Magnino, S., Bandi, C., 2008.

492   *Midichloria mitochondrii* is widespread in hard ticks (Ixodidae) and resides in the

493   mitochondria of phylogenetically diverse species. Parasitology 135, 485–494.

494   https://doi.org/10.1017/S0031182007004052

495 Guizzo, M.G., Neupane, S., Kucera, M., Perner, J., Frantová, H., da Silva Vaz, I.J., Oliveira,

496   P.L. de, Kopacek, P., Zurek, L., 2020. Poor Unstable Midgut Microbiome of Hard

497   Ticks Contrasts With Abundant and Stable Monospecific Microbiome in Ovaries.

498   Front. Cell. Infect. Microbiol. 10. https://doi.org/10.3389/fcimb.2020.00211

499 Guizzo, M.G., Parizi, L.F., Nunes, R.D., Schama, R., Albano, R.M., Tirloni, L., Oldiges, D.P.,

500   Vieira, R.P., Oliveira, W.H.C., Leite, M. de S., Gonzales, S.A., Farber, M., Martins,

501   O., Vaz, I. da S., Oliveira, P.L., 2017. A *Coxiella* mutualist symbiont is essential to the

502   development of *Rhipicephalus microplus*. Sci. Rep. 7, 1–10.

503   https://doi.org/10.1038/s41598-017-17309-x

504 Jia, N., Wang, J., Shi, W., Du, L., Sun, Y., Zhan, W., Jiang, J.-F., Wang, Q., Zhang, B., Ji, P.,

505   Bell-Sakyi, L., Cui, X.-M., Yuan, T.-T., Jiang, B.-G., Yang, W.-F., Lam, T.T.-Y.,

506   Chang, Q.-C., Ding, S.-J., Wang, X.-J., Zhu, J.-G., Ruan, X.-D., Zhao, L., Wei, J.-T.,

507   Ye, R.-Z., Que, T.C., Du, C.-H., Zhou, Y.-H., Cheng, J.X., Dai, P.-F., Guo, W.-B.,

508   Han, X.-H., Huang, E.-J., Li, L.-F., Wei, W., Gao, Y.-C., Liu, J.-Z., Shao, H.-Z., Wang,

509   X., Wang, C.-C., Yang, T.-C., Huo, Q.-B., Li, W., Chen, H.-Y., Chen, S.-E., Zhou, L.-

510   G., Ni, X.-B., Tian, J.-H., Sheng, Y., Liu, T., Pan, Y.-S., Xia, L.-Y., Li, J., Zhao, F.,

511   Cao, W.-C., 2020. Large-Scale Comparative Analyses of Tick Genomes Elucidate

512   Their Genetic Diversity and Vector Capacities. Cell 182, 1328-1340.e13.

513   https://doi.org/10.1016/j.cell.2020.07.023

514 Jongejan, F., Uilenberg, G., 2004. The global importance of ticks. Parasitology 129, S3–S14.

515   https://doi.org/10.1017/S0031182004005967Kahl, O., Hoff, R., Knülle, W., 1990.

516   Gross morphological changes in the salivary glands of *Ixodes ricinus* (Acari,

517   Ixodidae) between bloodmeals in relation to active uptake of atmospheric water

518   vapour. Exp. Appl. Acarol. 9, 239–258. https://doi.org/10.1007/BF01193431

519   Lo, N., Beninati, T., Sassera, D., Bouman, E. a. P., Santagati, S., Gern, L., Sambri, V.,

520   Masuzawa, T., Gray, J.S., Jaenson, T.G.T., Bouattour, A., Kenny, M.J., Guner, E.S.,

521   Kharitonenkov, I.G., Bitam, I., Bandi, C., 2006. Widespread distribution and high

522   prevalence of an alpha-proteobacterial symbiont in the tick *Ixodes ricinus*. Environ.

523   Microbiol. 8, 1280–1287. https://doi.org/10.1111/j.1462-2920.2006.01024.x

524   Mariconti, M., Epis, S., Gaibani, P., Valle, C.D., Sassera, D., Tomao, P., Fabbi, M., Castelli,

525   F., Marone, P., Sambri, V., Bazzocchi, C., Bandi, C., 2012. Humans parasitized by

526   the hard tick *Ixodes ricinus* are seropositive to *Midichloria mitochondrii*: is *Midichloria*

527   a novel pathogen, or just a marker of tick bite? Pathog. Glob. Health 106, 391–396.

528   https://doi.org/10.1179/2047773212Y.0000000050

529   Narasimhan, S., Fikrig, E., 2015. Tick microbiome: the force within. Trends Parasitol. 31,

530   315–323. https://doi.org/10.1016/j.pt.2015.03.010

531   Ogle, D.H., Wheeler, P., Dinno, A., 2020. FSA: Fisheries Stock Analysis.

532   Oliver, J.H., 1977. Cytogenetics of Mites and Ticks. Annu. Rev. Entomol. 22, 407–429.

533   https://doi.org/10.1146/annurev.en.22.010177.002203

534   Olivieri, E., Epis, S., Castelli, M., Varotto Boccazzi, I., Romeo, C., Desirò, A., Bazzocchi, C.,

535   Bandi, C., Sassera, D., 2019. Tissue tropism and metabolic pathways of *Midichloria*

536   *mitochondrii* suggest tissue-specific functions in the symbiosis with Ixodes ricinus.

537   Ticks Tick-Borne Dis. 10, 1070–1077. https://doi.org/10.1016/j.ttbdis.2019.05.019

538   Parola, P., Raoult, D., 2001. Tick-borne bacterial diseases emerging in Europe. Clin.

539   Microbiol. Infect. 7, 80–83. https://doi.org/10.1046/j.1469-0691.2001.00200.x

540   R Core Team, 2020. R: A Language and Environment for Statistical Computing. R

541   Foundation for Statistical Computing, Vienna, Austria.

542   Sacchi, L., Bigliardi, E., Corona, S., Beninati, T., Lo, N., Franceschi, A., 2004. A symbiont of

543   the tick *Ixodes ricinus* invades and consumes mitochondria in a mode similar to that

544   of the parasitic bacterium *Bdellovibrio bacteriovorus*. Tissue Cell 36, 43–53.

545   https://doi.org/10.1016/j.tice.2003.08.004

546   Sassera, D., Beninati, T., Bandi, C., Bouman, E.A.P., Sacchi, L., Fabbi, M., Lo, N., 2006.

547   '*Candidatus* Midichloria mitochondrii', an endosymbiont of the tick Ixodes ricinus with

548   a unique intramitochondrial lifestyle. Int. J. Syst. Evol. Microbiol. 56, 2535–2540.

549   https://doi.org/10.1099/ijs.0.64386-0

550   Sassera, D., Lo, N., Bouman, E.A.P., Epis, S., Mortarino, M., Bandi, C., 2008. "Candidatus

551   *Midichloria*" Endosymbionts Bloom after the Blood Meal of the Host, the Hard Tick

552   *Ixodes ricinus*. Appl. Environ. Microbiol. 74, 6138–6140.

553   https://doi.org/10.1128/AEM.00248-08

554   Stavru, F., Riemer, J., Jex, A., Sassera, D., 2020. When bacteria meet mitochondria: The

555   strange case of the tick symbiont *Midichloria mitochondrii*. Cell. Microbiol. 22,

556   e13189. https://doi.org/10.1111/cmi.13189

557   Vautrin, E., Vavre, F., 2009. Interactions between vertically transmitted symbionts:

558   cooperation or conflict? Trends Microbiol. 17, 95–99.

559   https://doi.org/10.1016/j.tim.2008.12.002

560   Wickham, H., 2016. ggplot2: Elegant Graphics for Data Analysis. Springer-Verlag New York.

561   Wickham, H., François, R., Henry, L., Müller, K., 2020. dplyr: A Grammar of Data

562   Manipulation.

563   Wickham, H., Henry, L., 2020. tidyr: Tidy Messy Data.

564   Wilke, C.O., 2019. cowplot: Streamlined Plot Theme and Plot Annotations for "ggplot2."

565   Zhang, C.-M., Li, N.-X., Zhang, T.-T., Qiu, Z.-X., Li, Y., Li, L.-W., Liu, J.-Z., 2017.

566   Endosymbiont CLS-HI plays a role in reproduction and development of

567   *Haemaphysalis longicornis*. Exp. Appl. Acarol. 73, 429–438.

568   https://doi.org/10.1007/s10493-017-0194-y

569   Zhong, J., Jasinskas, A., Barbour, A.G., 2007. Antibiotic Treatment of the Tick Vector

570   *Amblyomma americanum* Reduced Reproductive Fitness. PLOS ONE 2, e405.

571   https://doi.org/10.1371/journal.pone.0000405

572   Zhu, Z., Aeschlimann, A., Gern, L., 1992. *Rickettsia*-like microorganisms in the ovarian

573   primordial of molting *Ixodes ricinus* (Acari: Ixodidae) larvae and nymphs. Ann.

574   Parasitol. Hum. Comparée 67, 99–110. https://doi.org/10.1051/parasite/199267499

575 **Legends to figures**

576 **Fig. 1**. Experimental design and creation of the size groups ($x_{1,S}$, $x_{1,M}$, $x_{1,L}$). The size groups

577 were each subdivided into two groups, one to measure the *Midichloria* density at the unfed

578 stage (around one third of x_1, $x_{2,S}$, $x_{2,M}$, $x_{2,L}$), the other to perform the blood meal (around two

579 thirds of x_1, $x_{3,S}$, $x_{3,M}$, $x_{3,L}$). The x_3 groups were weighed then divided into two subgroups, one

580 to measure the *Midichloria* density at the fed stage (around half of x_3, $x_{4,S}$, $x_{4,M}$, $x_{4,L}$), the

581 other to determine the sex of the imago (around half of x_3, $x_{5,S}$, $x_{5,M}$, $x_{5,L}$).

582

583 **Fig. 2:** *Ixodes ricinus* nymph. Hypostome and scutum lengths were measured as indicated

584 by the grey arrows.

585

586 **Fig. 3**: Composition of the three groups (small, medium, large) based on the hypostome and

587 scutum length, measured at the unfed stage. Blue dots - small ($x_{1,S}$), green dots - medium

588 ($x_{1,M}$), red dots - large ($x_{1,L}$). ($R2 = 0{,}2819$, $P < 0.01$). The unit used for scutum and

589 hypostome lengths is 10^{-4} m.

590

591 **Fig. 4**: Ratio gyrB/cal indicating the *Midichloria mitochondrii* density, in the different unfed

592 nymph groups.

593

594 **Fig. 5:** Body mass of engorged nymphs. Sex determination of those nymphs corresponded

595 this time to the observed sex as it was based on the sex of the adults obtained after moulting

596 of engorged nymphs (that were weighed prior to metamorphosis).

597

598 **Fig. 6** : Density estimator of the body mass (a) with all engorged nymphs from the 3 groups

599 (small, medium, large) merged. The vertical line indicates the minimum between the two
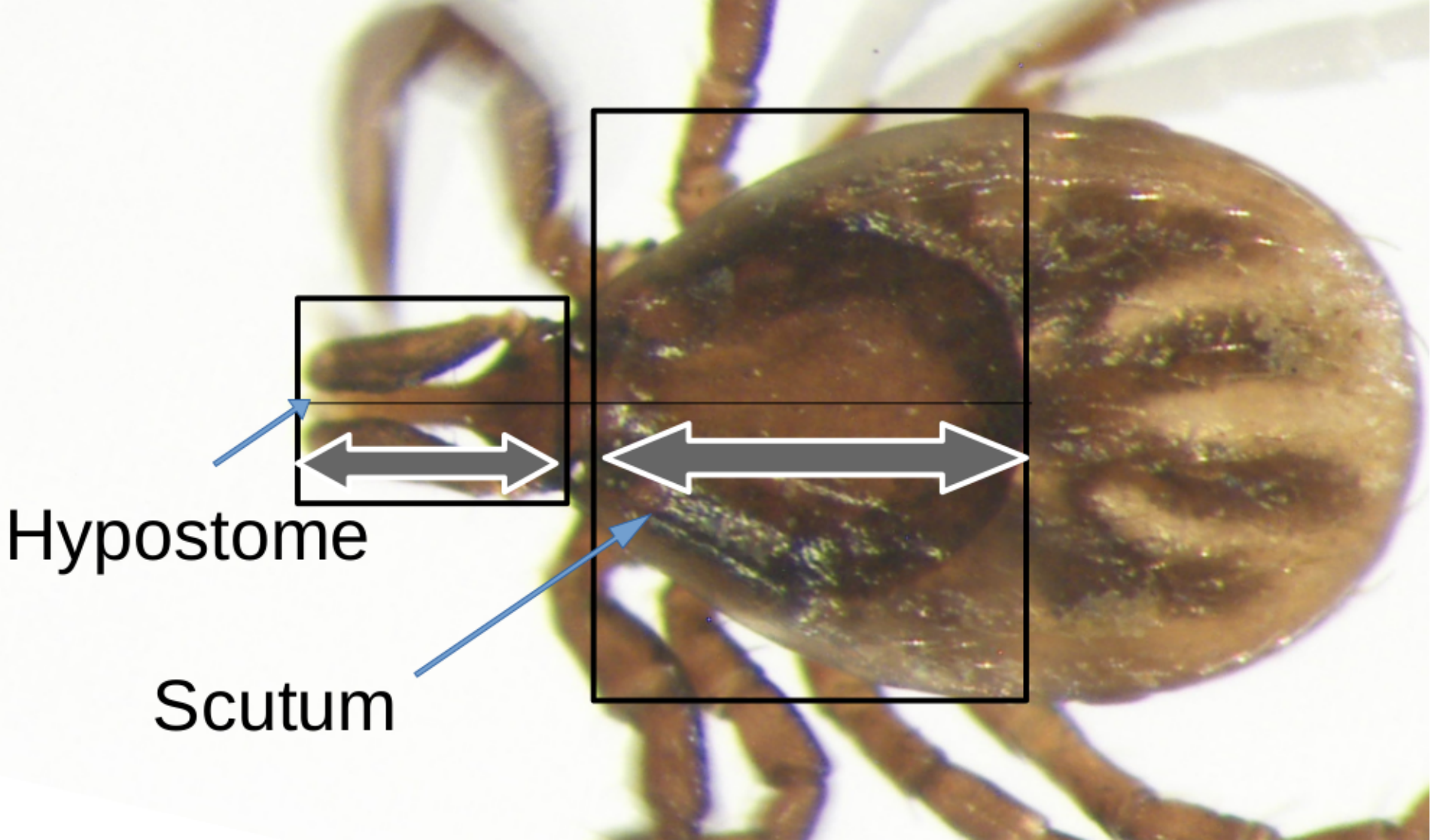
600 modes (body mass = 3.78).

601

602 **Fig. 7**: Violin plot of the body mass according to the fed nymph groups.

603

604   **Fig. 8**: Individual gyrB/cal ratios of fed nymphs in the three size groups.
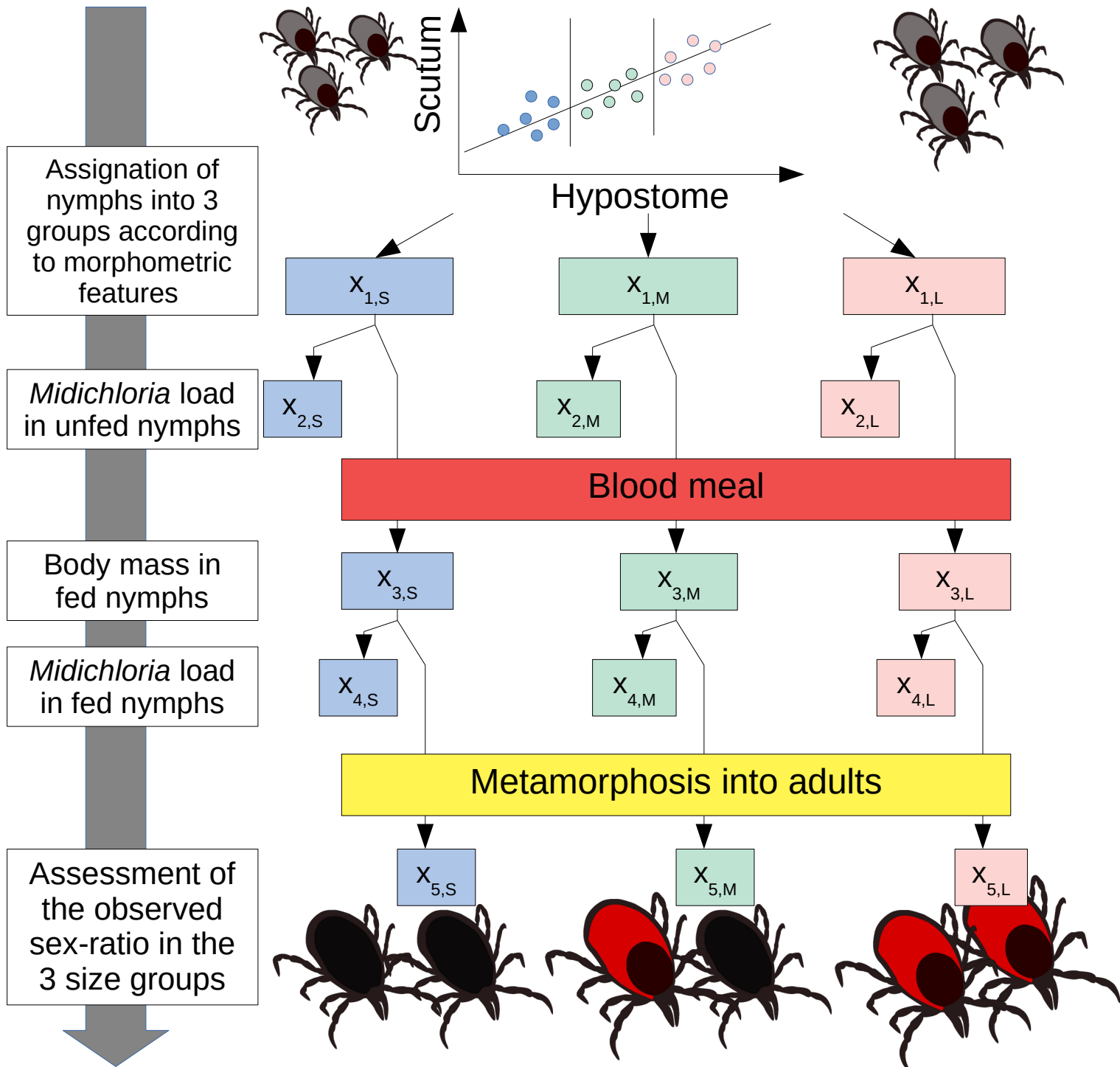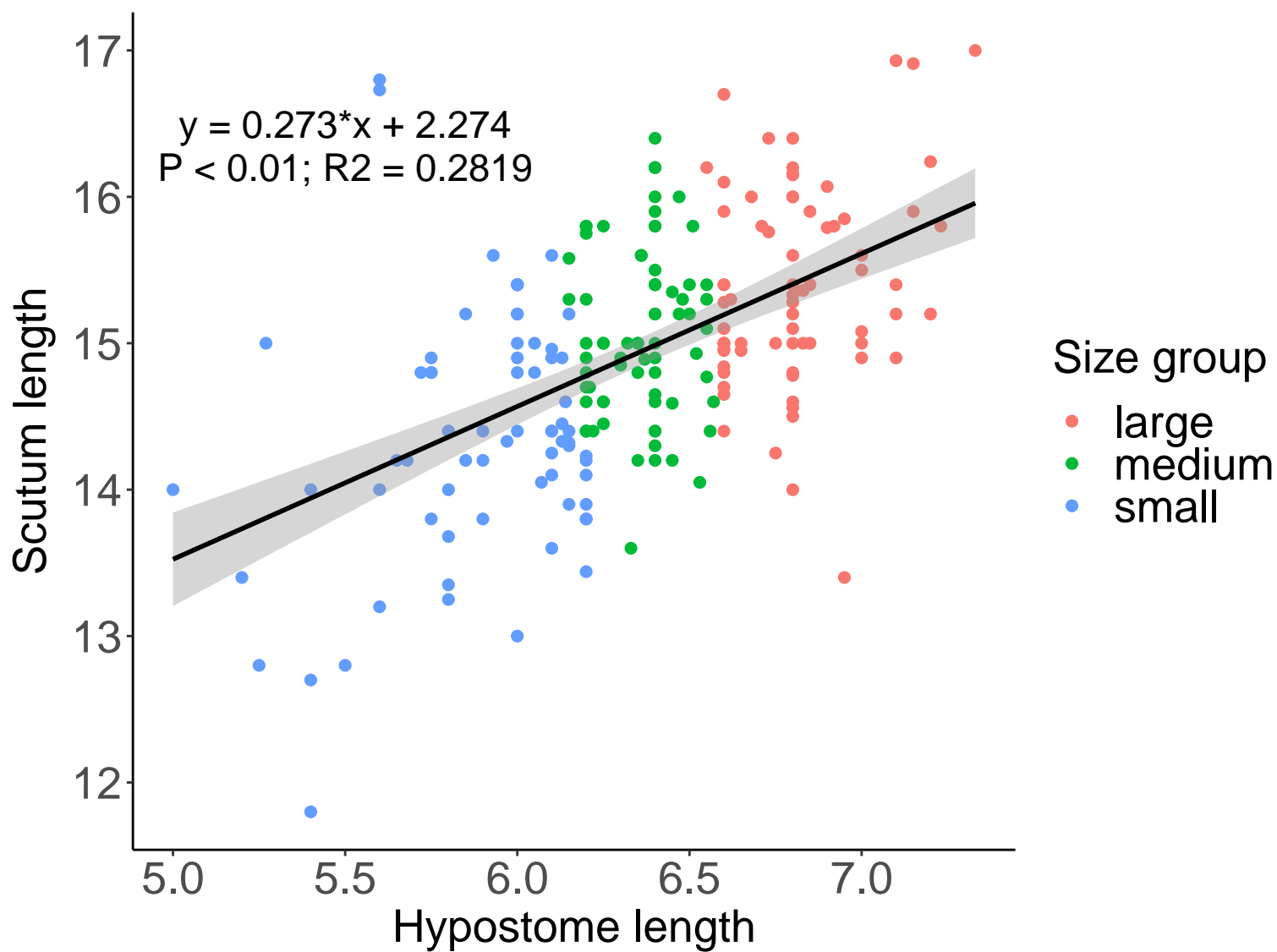
605

606   **Fig. 9**: Relationship between fed body mass and *Midichloria* density (gyrB/cal ratio) for fed

607   nymphs of *I. ricinus*. Ellipses were made using the stat_ellipse() function of the ggplot
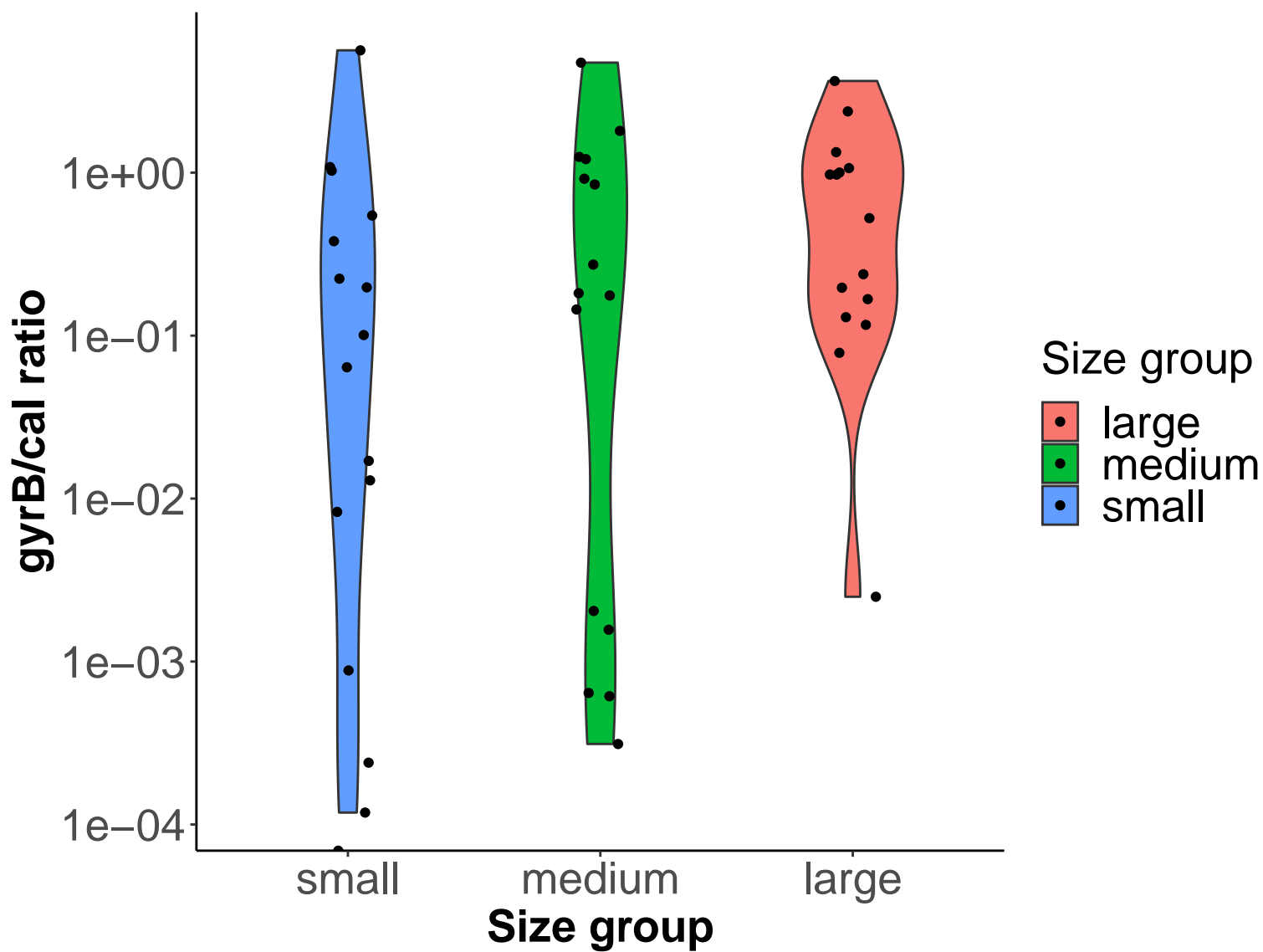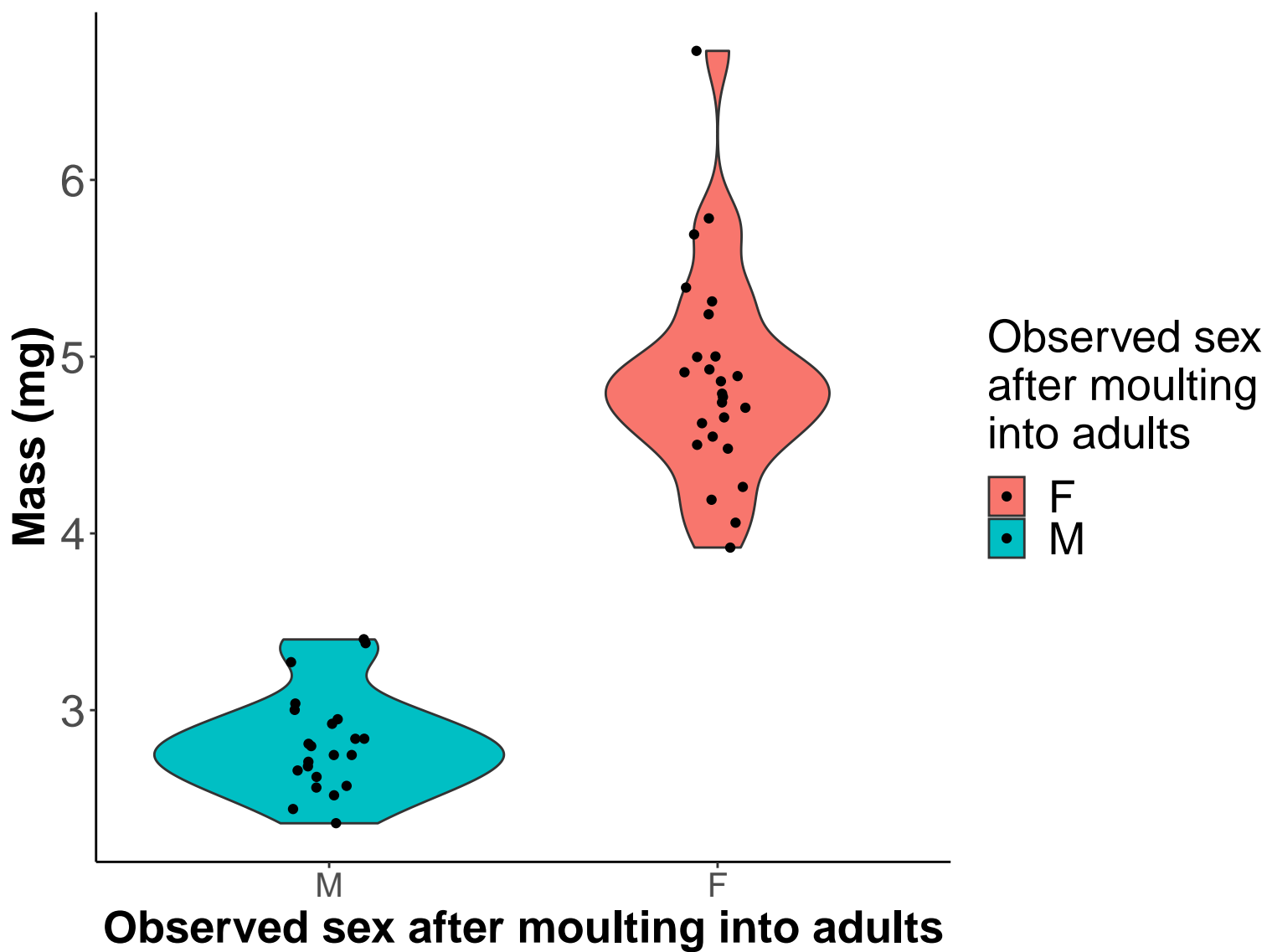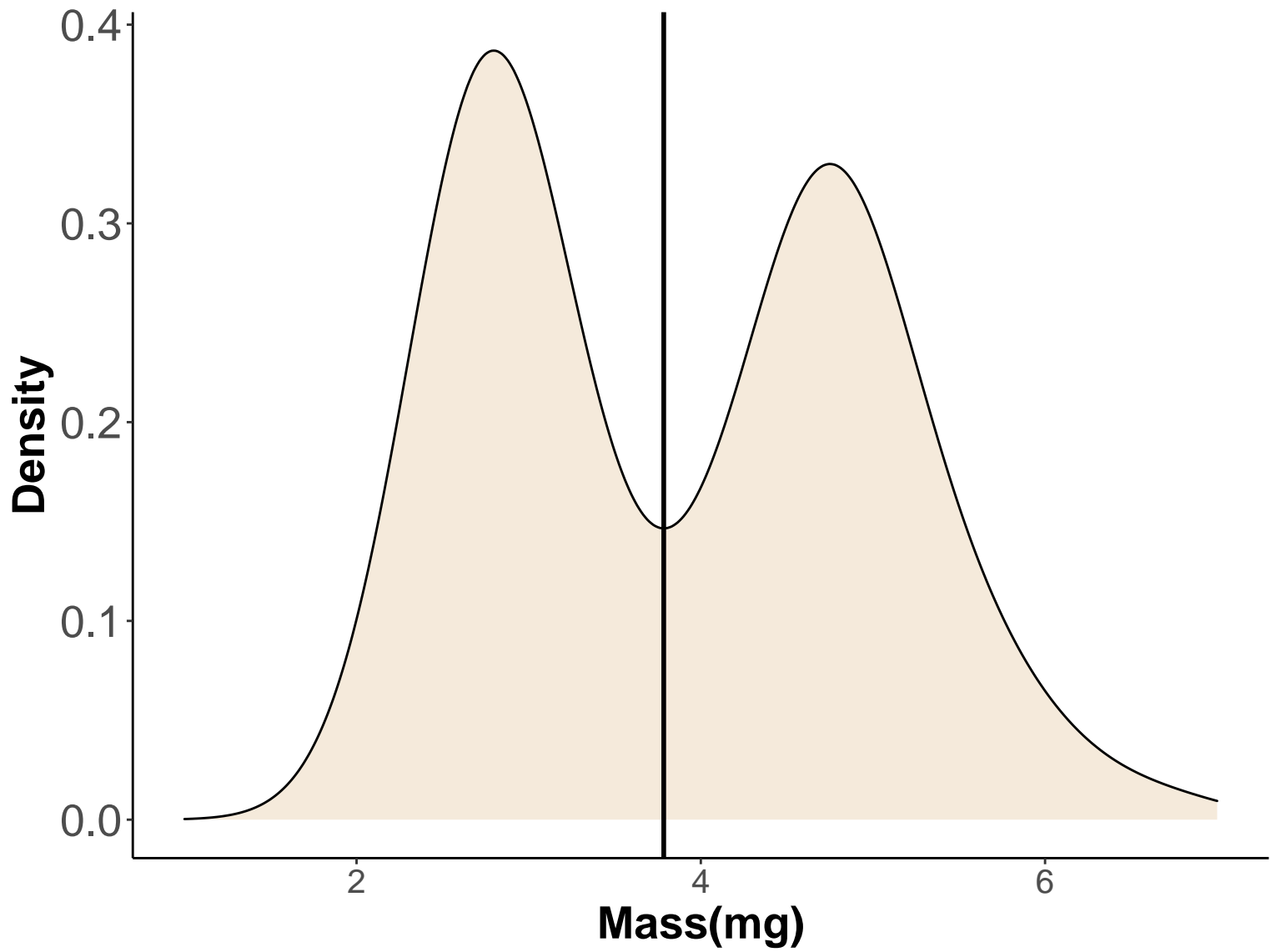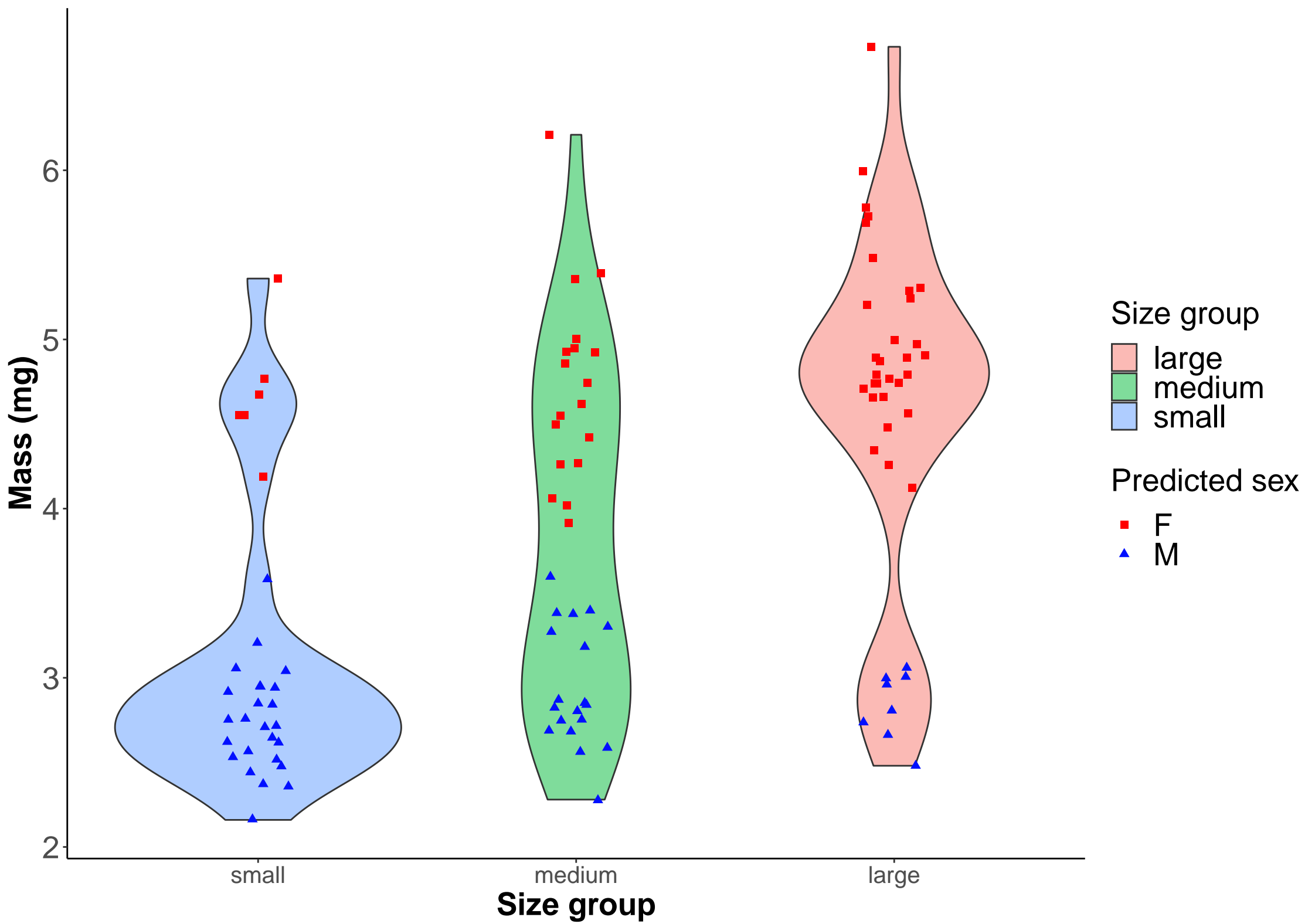
608   package.

Hypostome

Scutum

Assignation of nymphs into 3 groups according to morphometric features

Scutum

Hypostome

$X_{1,S}$

$X_{1,M}$

$X_{1,L}$

Midichloria load in unfed nymphs

$X_{2,S}$

$X_{2,M}$

$X_{2,L}$

Blood meal

Body mass in fed nymphs

$X_{3,S}$

$X_{3,M}$

$X_{3,L}$

Midichloria load in fed nymphs

$X_{4,S}$

$X_{4,M}$

$X_{4,L}$

Metamorphosis into adults

Assessment of the observed sex-ratio in the 3 size groups

$X_{5,S}$

$X_{5,M}$

$X_{5,L}$
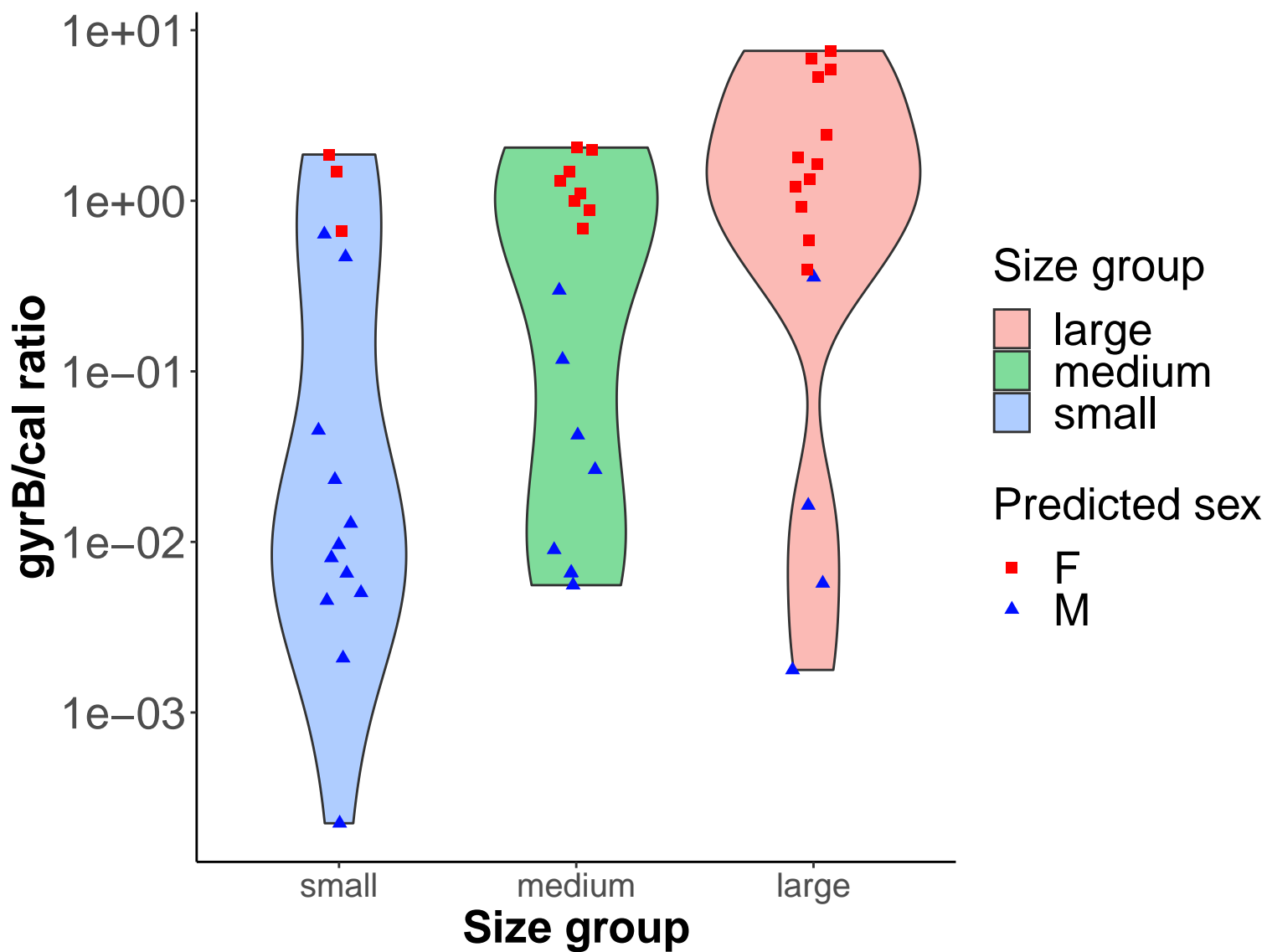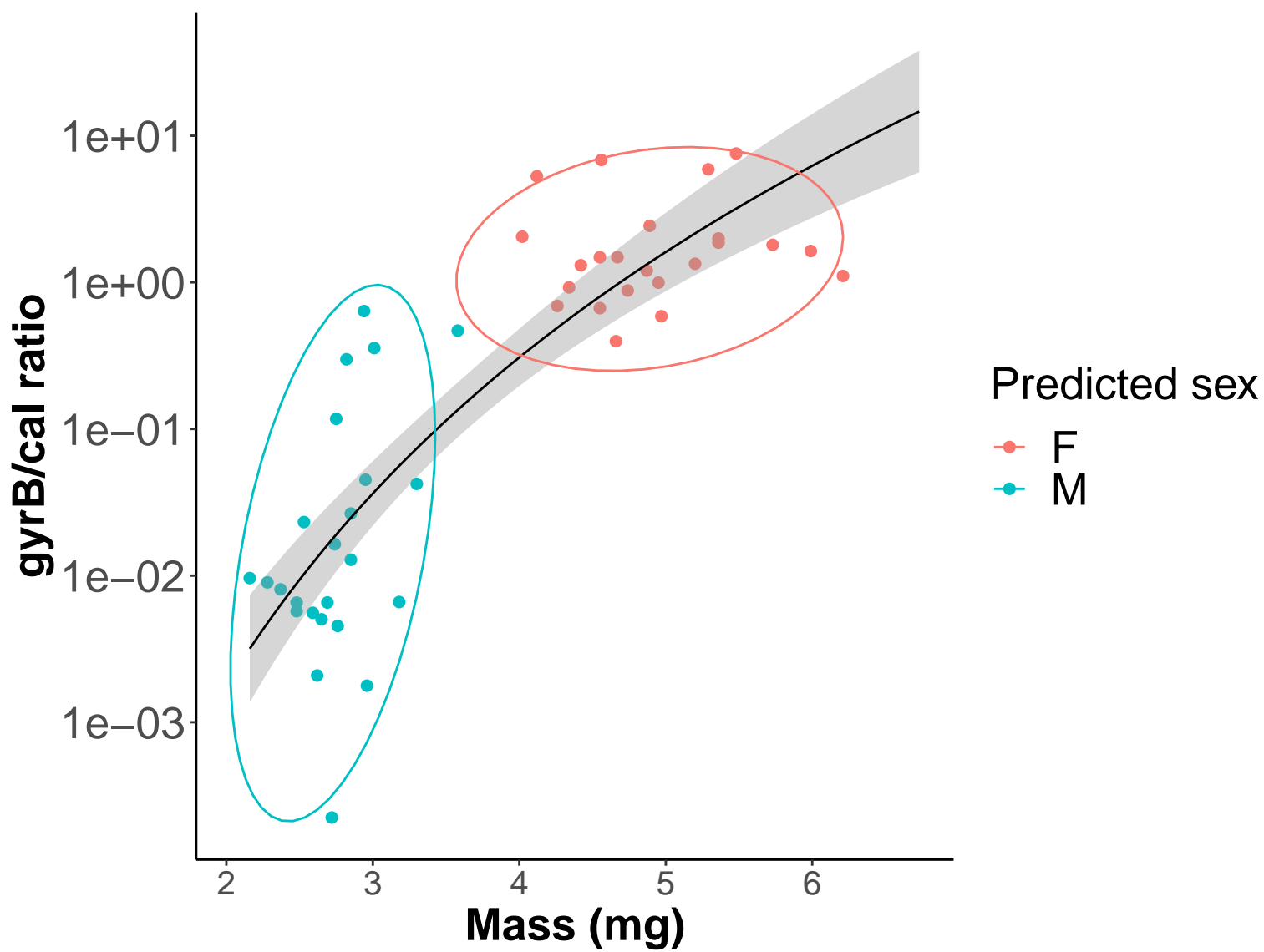
Group	qPCR unfed	Failed to feed	qPCR fed	Moulted to adults $= x_{5,S/M/L}$		Died during moulting	Total
				Female	Male		
Small (S)	$x_{2,S} = 18$	16	$x_{4,S} = 16$	2	11	2	$x_{1,S} = 65$
Medium (M)	$x_{2,M} = 15$	13	$x_{4,M} = 19$	8	8	2	$x_{1,M} = 65$
Large (L)	$x_{2,L} = 15$	12	$x_{4,L} = 19$	15	3	1	$x_{1,L} = 65$
Total	$x_2 = 48$	41	$x_4 = 54$	25	22	5	$x_1 = 195$